

Towards Granularity-adjusted Pixel-level Semantic Annotation

Rohit Kundu¹, Sudipta Paul², Rohit Lal¹, Amit K. Roy-Chowdhury¹

¹University of California, Riverside ²Samsung Research America

{rkund006@, spaul007@, rlal011@, amitrc@ece.}ucr.edu

Abstract

Recent advancements in computer vision predominantly rely on learning-based systems, leveraging annotations as the driving force to develop specialized models. However, annotating pixel-level information, particularly in semantic segmentation, presents a challenging and labor-intensive task, prompting the need for autonomous processes. In this work, we propose GranSAM which distinguishes itself by providing semantic segmentation at the user-defined granularity level on unlabeled data without the need for any manual supervision, offering a unique contribution in the realm of semantic mask annotation method. Specifically, we propose an approach to enable the Segment Anything Model (SAM) with semantic recognition capability to generate pixel-level annotations for images without any manual supervision. For this, we accumulate semantic information from synthetic images generated by the Stable Diffusion model or web crawled images and employ this data to learn a mapping function between SAM mask embeddings and object class labels. As a result, SAM, enabled with granularity-adjusted mask recognition, can be used for pixel-level semantic annotation purposes. We conducted experiments on the PASCAL VOC 2012 and COCO-80 datasets and observed a +17.95% and +5.17% increase in mIoU, respectively, compared to existing state-of-the-art methods when evaluated under our problem setting.

1. Introduction

Data has been the driving factor of the modern deep learning era. A tremendous amount of effort goes into annotating unlabeled data so that specialized models can be trained in a supervised fashion [29], enabling various task capabilities. However, it becomes expensive when we need to annotate every pixel of an image or generate semantic masks. In this work, our goal is to develop a system that can automatically generate pixel-level annotations/semantic masks for the desired object categories without any manual supervision. Towards that goal, we introduce a novel annotation framework that builds upon the Segment Anything Model (SAM) [9],

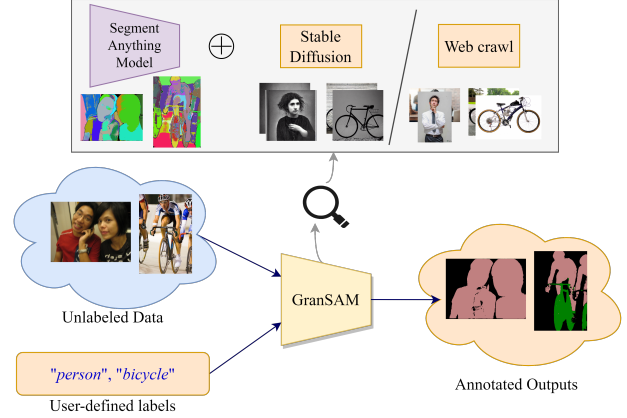


Figure 1. **Problem Overview:** Given a set of unlabeled images and a set of object classes a user needs to annotate, our proposed GranSAM can generate pixel-level semantic annotation without any manual supervision. We develop GranSAM by enabling SAM with semantic region recognition capability utilizing synthetic images generated by Stable Diffusion or images collected from web for the desired object classes.

the overview of which is shown in Figure 1.

SAM [9], a promptable foundation model designed for segmentation tasks, demonstrates proficiency in generating segmentation masks at various granularities based on input prompts, such as point or bounding box annotations, owing to its supervised large-scale pretraining. However, SAM lacks object semantics awareness. To address this limitation, we enhance SAM to provide pixel-level annotations for user-specified classes without using manual labels. This enhancement is achieved through the incorporation of a classifier head on SAM, trained using synthetic images generated via Stable Diffusion model [20] or web crawled images, capturing essential semantic information.

The integration of a classifier head, developed on SAM’s mask decoder, plays a crucial role in automating the generation of semantic segmentation masks with object-label annotations. Unlike traditional unsupervised methods [4, 17, 26, 31] that require a large-scale in-distribution unlabeled data to learn pixel-level representation or adaptation

to target unlabeled data, our GranSAM framework strategically overcomes this limitation. By utilizing domain agnostic mask embeddings of SAM, the classifier trained with set of images obtained through Stable Diffusion or by crawling the web, seamlessly transfer to images of different distributions, ensuring robust performance. This unique feature positions our framework as a practical and versatile solution for semantic segmentation based annotation systems.

Our proposed GranSAM (SAM, adapted to the granularity of user-defined classes) model distinguishes itself by adopting a user-centric approach to semantic segmentation. In contrast to SAM, which generates numerous unlabeled masks, our strategy is focused and meaningful. Rather than overwhelming users with an excess of masks, GranSAM specifically provides targeted masks for user-defined objects, accompanied by meaningful labels. This user-centric methodology optimizes the segmentation process, aligning with real-world scenarios where users typically seek specific objects within an image. By tailoring the granularity of object masks to the user’s specific needs, this approach enhances the overall usability of the segmentation results.

Following are the contributions of the work:

- We propose GranSAM, a novel semantic segmentation based annotation framework that does not require any manually labeled images or human interaction.
- We introduce a unique approach to enhance SAM, enabling it to recognize masks at the desired granularity based on semantic information. Leveraging Stable Diffusion model or web, we collect a set of images containing user defined classes. These images guide SAM to identify predicted masks at the desired granularity.
- Our empirical results demonstrate superior performance compared to state-of-the-art unsupervised semantic segmentation methods trained using Stable Diffusion-generated synthetic images or web crawled images.

2. Related Work

Efficient Annotation: Efficient annotation methods aim to reduce the time and cost associated with the annotation process while maintaining or improving annotation quality. There are few works [2, 12] that uses human-in-the-loop to generate image-level annotation efficiently. Interactive object segmentation methods [1, 14] propose coarse segmentation masks which are then iteratively corrected by collecting point annotations (object vs background) from a human annotator. However, to the best of our knowledge, the research area for developing semantic segmentation annotation framework without access to any manual supervision remains unexplored.

Unsupervised Semantic Segmentation: Unsupervised semantic segmentation [4, 7, 17, 22, 26, 30, 31] entails the segmentation of an image into meaningful regions without

the reliance on labeled training data. Researchers have investigated diverse approaches to tackle this challenge, incorporating methods from unsupervised learning, clustering, and self-supervised learning. MaskContrast [24] stands out as an approach that performs unsupervised semantic segmentation within a contrastive learning framework. It assigns labels to the predicted clusters using Hungarian matching, optimizing test-time performance metrics by associating labels with clusters that maximize segmentation accuracy. ACSeg [11] is a state-of-the-art method, wherein they employed a pre-trained ViT model to mine “concepts” from the pixel representation space of the unlabeled training images. Unlike previous methods, ACSeg does not predefine the number of clusters an image will be partitioned into. Instead, they adaptively conceptualize on different images due to varying complexity in individual images.

However, these existing unsupervised methods assume access to a large unlabeled training dataset. This contrasts with our problem formulation, where we assume a scenario without access to such unlabeled data. In our approach, we operate under the assumption that we lack prior knowledge of the specific data distribution the user requires for annotation. We perform on-the-fly inference with our GranSAM model directly on the user’s data, eliminating the need for pre-existing knowledge of the data distribution.

SAM Variants: Several methods that build on SAM’s capabilities have been developed recently. SemanticSAM [10] is a fully supervised method that segments and recognizes open-set objects at any granularity, and is trained on a combination of the SA-1B dataset [9] with other panoptic and part-segmentation datasets. RegionSpot [27] leverages the SAM model and CLIP’s [18] Vision-Language feature embeddings to perform object detection. However, the method is dependent on (unlabeled) box annotations for every image, necessitating a comprehensive annotation effort for each object category. Grounded-SAM [19] and LangSAM [16] are two similar open-source projects based on SAM which aim to segment and detect anything with natural language prompts. However, it uses GroundingDINO [15] to detect objects where the model has been trained in a supervised fashion using object-level box annotations. In our work, we do not utilize such object detectors as they require additional object-level annotation effort.

3. Methodology

First, we formally define the problem statement (3.1) and present our GranSAM’s framework overview (3.2). Then we briefly explain SAM’s architecture (3.3) and describe our strategy to collect semantic information of different classes of interest (3.4). Finally, we explain how the collected semantic information is linked with mask embeddings of SAM to develop our annotation system (3.5) and the inference steps of the annotation system (3.6).

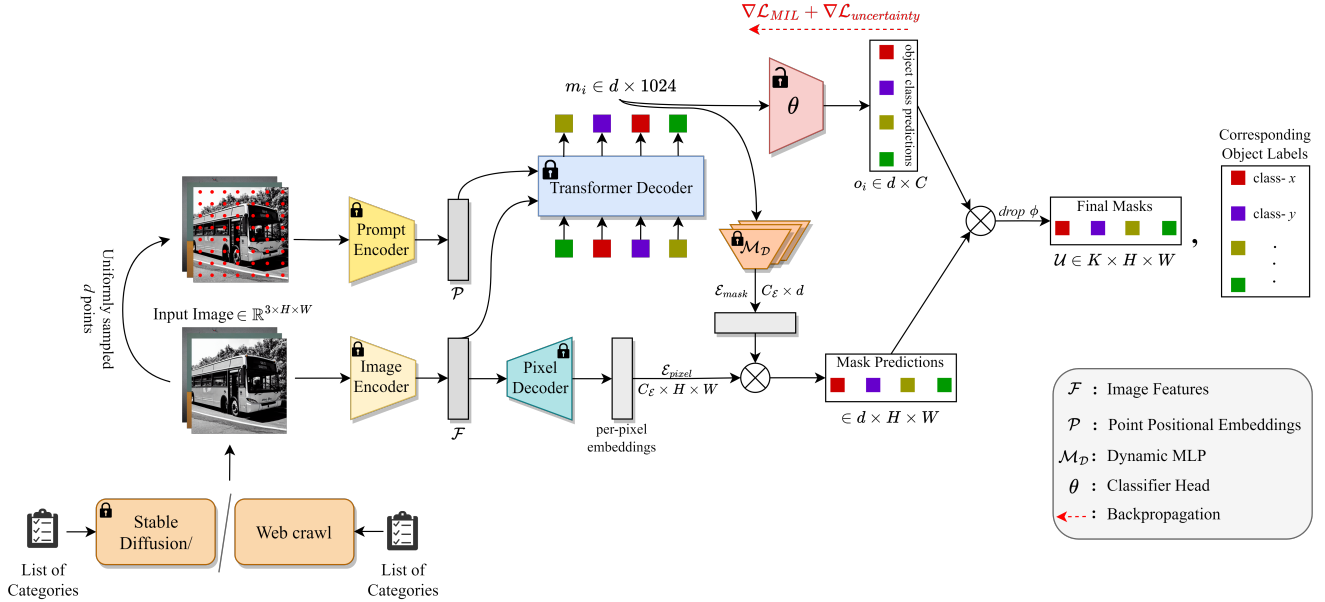


Figure 2. Overall workflow of GranSAM: Given the list of user-defined target categories \mathcal{C} , we use Stable Diffusion [21] to generate a synthetic single-object image dataset which is encoded by SAM’s [9] image encoder and a uniformly spaced grid of d points are generated across the image to prompt SAM. The image and point embeddings are passed into a transformer decoder, the output mask embeddings m_i (here, $m_i \in \mathbb{R}^{d \times 1024}$, corresponding to the d masks predicted by SAM) of which are used to train a classifier head θ to predict objects using a Multiple Instance Learning (MIL) setup and uncertainty losses (ref. Section 3.5).

3.1. Problem Statement

Consider, we have a set of unlabeled N images $\mathcal{X} = \{x_i\}_{i=1}^N$ where, $x_i \in \mathbb{R}^{H \times W \times 3}$. Given a set of $C + 1$ target classes $\mathcal{C} = \{c_i\}_{i=0}^C$ (C object classes and one background class), our objective is to generate semantic masks $\mathcal{U} = \{u_i\}_{i=1}^N$ for the unlabeled N images. Here, $s_i \in \mathcal{C}^{H \times W}$ and each image can contain variable number of objects. We also consider that apart from \mathcal{X} , we do not have access to more unlabeled images from the same distribution for unsupervised/self-supervised training purpose.

3.2. Framework Overview

To generate semantic segmentation masks, the system needs to be able to distinguish different regions of an image and understand the semantics of those regions simultaneously. We leverage domain agnostic Segment Anything Model (SAM) as the backbone of the system to distinguish the regions. Although SAM can generate masks at any granularity based on input prompts, it does not have the semantic understanding of the objects present in an image. To guide the semantic understanding, we utilize Stable Diffusion generated synthetic images/web crawled images of our classes of interest. Since, we know the image-level labels of the synthetic or web crawled images, we train a classifier head on top of SAM’s mask decoder in a weakly-supervised setup. For every generated mask of SAM, we parse the mask em-

bedding and map it to class labels using MLP layers. We use multiple instance learning loss to learn the mapping function. Since, SAM mask embeddings are domain agnostic, our learned classifier is also robust to distribution shifts and can be directly applicable to the unlabelled dataset of interest. Figure 2 provides a detailed architectural overview.

3.3. Segment Anything Model Architecture

Segment Anything Model (SAM) [9] is a foundation model for image segmentation task trained on a dataset consisting of 11M images and 1B masks. It can generate segmentation masks for images at varying granularity levels based on input prompts. It consists of three main parts:

Image Encoder. The input images are processed using a pre-trained Vision Transformer [5] modified to handle high resolution images of dimension $\mathbb{R}^{3 \times 1024 \times 1024}$. It is run once per image to obtain features of dimension $\mathbb{R}^{256 \times 64 \times 64}$ and can be applied prior to prompting the model.

Prompt Encoder. SAM takes sparse prompt inputs in the form of point or box annotations for mask inference. Alternatively, in SAM’s “automatic” mode, users don’t need to manually define points or bounding boxes in the image; instead, a uniformly spaced grid of points (say, ‘ d ’ number of total points; $d = 100$ for our case) is generated throughout the image which are used as point annotations to prompt SAM. These point prompts are represented as positional

embeddings summed with the corresponding learned embeddings (that indicates if a point is in the foreground or background) in SAM. Since, we do not have any prior information on where the object of interest is located, we use this “*automatic*” mode to generate all possible masks.

Mask Decoder. SAM’s mask decoder consists of a modified Transformer Decoder block [25] followed by a dynamic mask prediction heads. It maps the image and prompt embeddings along with an output token to a mask. A learned output token embedding which is analogous to the [class] token in [5], is first inserted into the set of prompt embeddings. This, along with the image embeddings are given as input to the transformer decoder that updates the output token embeddings (denoted by $m_{tokens} \in \mathbb{R}^{d \times 4 \times 256}$). The image embeddings are upscled by $4 \times$ and a point-wise product is taken with the output of a 3-layer MLP whose inputs are m_{tokens} . This product is the mask prediction of SAM, and this is performed for all of the d prompts (point annotations) resulting in a set of d binary masks $\in \mathbb{Z}_2^{d \times 256 \times 256}$ for each image.

3.4. Fetching Semantic Information

Although, SAM can predict masks by distinguishing different regions of the image, it does not have semantic understanding of the predicted masks. To enable SAM with recognition capability of user defined classes, we collect semantic information of those classes using synthetic images or web crawled images.

Synthetic Images. We use the Stable Diffusion [21] model which can generate hyper-realistic images given a text prompt. For each of the user-defined object classes in \mathcal{C} , we use the text prompt “a photo of a {c}” $\forall c \in \mathcal{C}$ and generate 200 single object images. This synthetic single-object image dataset serves as guide to enable semantic understanding for Segment Anything Model.

Web Crawled Images. Alternative to synthetic images, we can also use web crawled images for the same purpose. Through web crawling, we acquire single-object images for each user-defined object class in \mathcal{C} by utilizing them as search queries on the web. The web crawled images serve as a valuable addition to the training data, providing diversity in backgrounds and object contexts. This approach enhances the model’s ability to generalize across various visual scenarios and improves its discriminatory capacity for user-defined object classes.

3.5. Enabling Semantic Recognition

The d masks generated by SAM for each image contains semantic maps at all granularity and also includes background. Our objective is to identify mask(s) containing the desired object(s) specified by the user.

We introduce a classifier head, denoted as θ , designed to process SAM’s flattened mask embeddings $m \in \mathbb{R}^{d \times 1024}$.

θ is a simple 4-layer MLP network. The output of this classifier head $o_i = \theta(m_i)$, where $o_i \in \mathbb{R}^{d \times C}$ corresponds to the assigned object labels. In training the classifier head with the synthetic single-object training dataset, each image has a 1-dimensional object label (image-level label) within a d -dimensional input space (d mask embeddings per image). This unique characteristic necessitates us to use weakly supervised learning setup, leading to adopt a multiple-instance learning approach.

Multiple Instance Learning (MIL). In MIL, the d samples (SAM’s mask embeddings m_i for the i^{th} image) are grouped in ‘positive’ and ‘negative’ bags– ‘positive’ bags have at-least one positive instance (a mask embedding $m_i^j \in \mathbb{R}^{1 \times 1024}$ corresponding to the ground truth object label y_i) while ‘negative’ bags have no positive instances. Utilizing these bags as the training dataset, the objective is to train a model capable of not only classifying the entire bag but also distinguishing each individual instance within it as either a positive or negative sample.

To calculate the loss for each bag, denoted as the classifier output ‘ o_i ’ in our problem, we aim to express each d -dimensional mask embedding through a single confidence score for each category. For a set of mask embeddings associated with a given image, the activation score for a specific category is computed as the average of the k -max activations across the number of masks (d) for that category. In our case, the dimension $d = 100$ remains constant for all inputs, and we set k as,

$$k = \max \left(1, \left\lceil \frac{d}{a} \right\rceil \right), \quad (1)$$

where a is a design parameter. Thus, our class-wise confidence scores for the j^{th} class of the i^{th} input can be represented as,

$$s_i^j = \frac{1}{k} \max_{\substack{\mathcal{O} \subset \mathcal{O}_i[:,j] \\ |\mathcal{O}|=k}} \sum_{l=1}^k \mathcal{O}_l. \quad (2)$$

Subsequently, a softmax non-linearity is employed to derive the probability mass function across all categories as, $p_i^j = \frac{\exp(s_i^j)}{\sum_{j=1}^C \exp(s_i^j)}$. It is necessary to compare this probability mass function with the actual distribution of labels for each image to calculate the MIL loss. Since each image (during test-time) can have multiple objects in it, we represent the labels as a multi-hot vector, where 1 occurs if the object is present, else 0. We then normalize the ground truth label vector transforming it into a valid pmf. The MIL loss is subsequently computed as the cross-entropy between the predicted pmf, denoted as \mathbf{p}_i , and the normalized ground truth ($y_i = [y_i^1, \dots, y_i^C]^T$) as,

$$\mathcal{L}_{MIL} = \frac{1}{N} \sum_{i=1}^N \sum_{j=1}^C -y_i^j \log(p_i^j), \quad (3)$$

where N is the number of images and C is the number of object categories.

Uncertainty Distillation. To further improve the discriminative ability of the object classifier, we employ an Uncertainty Distillation setup by leveraging the uncertainty information during training. The MIL trained classifier from the previous stage acts as the teacher model θ_t (with parameters frozen), and the student model θ_s is an untrained classifier having the same architecture as θ_t . The primary motivation behind uncertainty distillation lies in enhancing the model’s ability to make well-calibrated predictions and acknowledge its own uncertainties in challenging scenarios.

For the mask embeddings of the i^{th} image, m_i , we compute the teacher logits as $o_i^t = \theta_t(m_i)$ and the teacher predictions as $\hat{y}_i^t = \text{argmax}(p_i^t)$, where $p_i^t = \text{softmax}(o_i^t) \in \mathbb{R}^{d \times C}$ are the object-label prediction probability scores for all the d masks. We calculate the entropy (uncertainty) in the teacher logits as $H_i^t = -\sum_{j=1}^C p_{ij}^t \cdot \log(p_{ij}^t)$. The goal is to minimize the reliance on (1) high entropy predictions, denoted by $H_i^{t,high}$, which are obtained by thresholding H_i^t (such that, $H_i^{t,high} = H_i^t > \text{threshold}$ and $H_i^{t,low} = H_i^t < \text{threshold}$), and (2) low entropy **incorrect** predictions, denoted as $H_i^{t,low,incorr} = H_i^{t,low} \cap \{\hat{y}_i^t \neq y_i\}$, where y_i is the ground truth object label. Thus, we obtain a set of bad predictions as $B_i = H_i^{t,high} \cup H_i^{t,low,incorr}$. Here, B_i represents the indices of the masks out of all the d masks predicted by SAM for the i^{th} image, where the classifier head predicts a label with highly uncertainty, or predicts a wrong label confidently.

Next, we obtain the student logits as $o_i^s = \theta_s(m_i)$ and compute the MIL loss, \mathcal{L}_{MIL} , as explained in the previous section. With the obtained bad teacher prediction indices, we compute the bad student logits as $o_i^{s,bad} = o_i^s[B_i, :]$. Finally, we compute the uncertainty loss (to be minimized) as,

$$\mathcal{L}_{uncertainty} = \frac{-1}{N} \sum_{i=1}^N \sum_{j=1}^C \log \left(\frac{\exp(o_{ij}^{s,bad})}{\sum_{j=1}^C \exp(o_{ij}^{s,bad})} \right). \quad (4)$$

The net loss used to guide the student model is a weighted sum of the MIL and uncertainty losses as, $\mathcal{L}_s = \lambda_1 \cdot \mathcal{L}_{MIL} + \lambda_2 \cdot \mathcal{L}_{uncertainty}$. The trained student model θ_s is used for inference on the test data.

3.6. Inference

For the images in the test set, we obtain the mask embeddings m_i from SAM in the same way as during training on synthetic / web crawled images. These embeddings are passed through our trained classifier head θ_s to acquire

object-class confidence scores for each mask within an image. By applying a predefined threshold to the confidence scores, we selectively retain masks whose object labels have been predicted with high probability. Among the selected subset masks for each image, certain masks may be redundant. We use Non-Maximal Suppression (NMS) to eliminate those overlapping masks and ensure the retention of masks only corresponding to distinct objects.

4. Experiments

4.1. Datasets

Our experiments involve two benchmark datasets for multi-object images: PASCAL VOC 2012 [6] and COCO-80 [13]. **PASCAL VOC:** This dataset comprises 1449 images with annotations for 20 object classes. Noteworthy for its diversity, each image may contain a single or multiple objects, making it a versatile benchmark for evaluating segmentation algorithms.

COCO-80: COCO-80, with 80 classes, presents a complex multi-object scene understanding challenge. Featuring diverse object categories and rich annotations, including instance-level segmentation masks, it goes beyond traditional semantic segmentation datasets. Its scenarios involve numerous objects, intricate interactions, and occlusions, offering a realistic representation of challenging real-world contexts.

4.2. Implementation Details

SAM’s automatic mask generation mode uniformly places a grid of d points across the image, and for GranSAM, we set $d = 100$. We extracted and saved all d predicted masks from SAM, with the mask embeddings ($m_i \in \mathbb{R}^{d \times 1024}$). This one-pass extraction process ensures efficient storage for subsequent use in our workflow. We generated 200 synthetic single object images per class using the StableDiffusion-v1-4 [21] model. We first train the classifier head (teacher) θ_t , with the MIL loss (\mathcal{L}_{MIL}) as the sole objective with batch size 64, learning rate 0.001 optimized with the Adam optimizer. With these same hyperparameters, we train the student model θ_s with the objective $\mathcal{L}_s = \lambda_1 \cdot \mathcal{L}_{MIL} + \lambda_2 \cdot \mathcal{L}_{uncertainty}$, where we set $\lambda_1 = 1$ and $\lambda_2 = 0.15$. For our entire workflow, we utilized a single NVIDIA GeForce RTX 3090 GPU.

4.3. Evaluation Metrics

Our quantitative evaluation of GranSAM relies on two key metrics: mean Intersection over Union (mIOU) and mean Average Precision at an IoU threshold of 50% (mAP₅₀). **mIoU:** This metric evaluates the overlap between predicted segmentation masks and ground truth masks for each object class. It calculates the per-class Intersection over Union (IoU) as the intersection area divided by the union area of

Table 1. **State-of-the-art** comparison with our results on the PASCAL VOC *val* data. Although methods like TransFGU [28] outperform GranSAM, they were trained on the unlabeled data PASCAL VOC *train* set. When TransFGU [28] and Leopart [32] were evaluated on our problem setting, they distinctly underperformed against GranSAM.

Method	Training Data			mIoU	mAP ₅₀
	PASCAL	Synthetic	Web crawl		
MoCO v2 [8]	✓			4.30%	-
InfoMin [23]	✓			3.70%	-
SWAV [3]	✓			4.40%	-
MaskContrast [24]	✓			35.00%	-
TransFGU [28]	✓			37.15%	-
ACSeg [11]	✓			47.10%	-
Leopart [32]		✓		7.21%	-
TransFGU [28]		✓		2.05%	-
GranSAM		✓		25.16%	49.06%
Leopart [32]			✓	6.79%	-
TransFGU [28]			✓	2.45%	-
GranSAM			✓	22.42%	45.59%

the predicted and ground truth masks. The average of these per-class IOU scores, mIoU, provides an overall measure of segmentation accuracy.

mAP₅₀: Commonly used in object detection and segmentation tasks, mAP₅₀ assesses object localization precision at a 50% IoU threshold. It calculates Average Precision (AP) for each class based on precision-recall curves, and mAP₅₀ averages these class-specific AP scores. This metric is crucial for evaluating the model’s ability to precisely locate objects with moderate overlap.

4.4. Experimental Analysis

Quantitative Results. In this section, we quantitatively analyze the performance of our proposed GranSAM for the semantic segmentation annotation task. Table 1 and Table 2 reports the performance of GranSAM and compare it with other existing state-of-the-art methods.

GranSAM is trained on synthetic/web-crawled data to recognize object semantics and applied for inference on the *val* sets of PASCAL VOC and COCO-80 datasets. While unsupervised semantic segmentation methods are a common choice for annotation without manual supervision, state-of-the-art unsupervised methods typically rely on large-scale unlabeled datasets from the same distribution as the test set. Given our assumption that we lack access to such large-scale unlabeled data from the same distribution, a fair comparison with existing state-of-the-art unsupervised methods is challenging. To establish a fair baseline for comparison, we setup two unsupervised methods, Leopart [32] and TransFGU [28], trained on our synthetic/web-crawled data and evaluated on the PASCAL VOC and COCO-80 datasets. In Tables 1 and 2, our focus is primarily on the performance of Leopart [32] and TransFGU [28] when trained on our synthetic/web-crawled data.

Table 1 presents the performance comparison between

Table 2. **State-of-the-art** comparison with our results on the COCO-80 *val* data. We observe that TransFGU [28] performance drops significantly when trained on synthetic or web crawled images (our problem setting) as compared to when trained with COCO *train* data, and GranSAM outperforms these methods in similar problem settings.

Method	Training Data			mIoU	mAP ₅₀
	COCO	Synthetic	Web crawl		
MaskContrast [24]	✓			3.73%	-
TransFGU [28]	✓			12.69%	-
ACSeg [11]	✓			16.40%	-
Leopart [32]		✓		3.84%	-
TransFGU [28]		✓		0.95%	-
GranSAM		✓		8.60%	30.90%
Leopart [32]			✓	3.81%	-
TransFGU [28]			✓	1.02%	-
GranSAM			✓	9.01%	31.80%

GranSAM and state-of-the-art methods on the PASCAL VOC dataset. Notably, GranSAM demonstrates competitive performance compared to established methods like MoCO v2 [8] and SWAV [3]. However, methods such as MaskContrast [24], TransFGU [28], and ACSIeg [11], trained on the *train* set of PASCAL VOC, outperform GranSAM. It’s essential to note that direct comparisons with these methods are challenging, as they utilize unlabeled data from the test data distribution. However, when TransFGU [28] and Leopart [32] are trained on our synthetic/web crawled data and tested on the PASCAL VOC *val* set, they perform poorly, indicating a lack of generalization when the training data does not align with the distribution of the test data.

Table 2 highlights the performance of GranSAM and existing state-of-the-art methods on the COCO-80 dataset. This dataset, characterized by its diverse set of 80 object classes and complex scenes, reveals a notable decrease in performance across all methods, including ours. Challenges inherent in COCO-80, such as diverse object sizes, occlusions, and intricate interactions, contribute to the difficulty of achieving high mIoU scores for state-of-the-art methods. Even so, when the state-of-the-art methods were trained on the synthetic/web crawled data and tested on the COCO-80 *val* set, the results are significantly poor compared to our GranSAM framework. The occurrence of a low mIoU and a high mAP₅₀ in the COCO-80 dataset in Table 2 suggests a trade-off between localization precision and segmentation accuracy. A high mAP₅₀ indicates the model’s proficiency in object detection and localization, while a low mIoU implies challenges in precisely delineating object boundaries or capturing fine-grained details.

It is essential to highlight a key aspect of our methodology: our training data originates from a small set of synthetic (200 images per class) or web crawled data (~45 images per class) which are single-object images, and thus distinctly different from the test data distribution. Unlike existing methods, which often rely on detailed annotations

Class → Dataset ↓	background	aeroplane	bicycle	bird	boat	bottle	bus	car	cat	chair	cow	diningtable	dog	horse	motorbike	person	pottedplant	sheep	sofa	train	tvmonitor
SD	79.73	0.05	29.88	14.96	7.34	34.21	54.05	47.47	9.40	5.12	21.12	6.09	15.21	8.64	44.26	60.03	16.56	14.15	11.12	26.68	22.26
WC	78.91	33.89	15.48	12.13	8.26	22.46	36.46	41.23	9.85	4.41	6.89	2.21	18.92	19.22	44.30	38.98	11.39	14.71	14.96	17.22	18.85

Table 3. Classwise mIoU (%) scores obtained by GranSAM on the PASCAL VOC dataset, when trained on (a) **SD**: Stable Diffusion generated synthetic images and (b) **WC**: Web crawled images.

Table 4. **Ablation study results on PASCAL VOC**: Uncertainty Distillation significantly improves performance in both synthetic and web crawled data training paradigms. MIL: Multiple Instance Learning.

Method	Training Data		mIoU	mAP ₅₀
	Synthetic	Web crawl		
MIL <i>only</i>	✓		22.42%	42.47%
MIL + Distillation	✓		25.16%	49.06%
MIL <i>only</i>		✓	17.42%	39.86%
MIL + Distillation		✓	22.42%	45.59%

for each image, our method only requires knowledge of the user-defined class names to be segmented across the entire dataset. The ability to apply an existing method to a new dataset, as achieved by GranSAM, without any knowledge of the distribution of the data in this dataset is a highly desired feature as it enhances generalizability well beyond what unsupervised domain adaptation can do.

Furthermore, the effectiveness of our method is evident in its ability to yield competitive results regardless of the data source, be it synthetic or web crawled images. When TransFGU [28] and Leopart [32] are trained on our synthetic or web crawled datasets, the performance drops significantly compared to their performance on in-distribution training data in both PASCAL VOC and COCO-80 datasets (GranSAM achieves +17.95% and +5.17% mIoU, compared to Leopart [32]), emphasizing the unique challenges posed by our problem setting. This flexibility underscores the robustness of our approach, allowing for practical applications in scenarios where obtaining extensive manual annotations per image is challenging or impractical.

Qualitative Results. In Figure 3, we present some qualitative results obtained by GranSAM. The example in Row-1 depicts a single-object image of class “sheep”, where SAM has provided several masks which includes background masks, wherein discrete grass patches in the image have also been segmented separately. Row-2 shows an example of a multi-object image where the objects are partially occluded by each other. Row-3 shows two objects belonging to the same class which are disconnected, while Row-4 shows an example where two objects belonging to the same class have a connected contour. In all of these

Table 5. **Ablation study results on COCO-80**: Uncertainty Distillation improves the performance marginally when θ is trained with synthetic images and significantly when it is trained with web crawled images. MIL: Multiple Instance Learning.

Method	Training Data		mIoU	mAP ₅₀
	Synthetic	Web crawl		
MIL <i>only</i>	✓		8.01%	30.89%
MIL + Distillation	✓		8.60%	30.97%
MIL <i>only</i>		✓	8.57%	27.57%
MIL + Distillation		✓	9.01%	31.81%

cases, GranSAM has been able to filter out the desired mask along with the correct object label whereas SAM has segmented several different parts of the image- both small and large objects, for example, the eyes and the faces have been segmented separately in Row-4.

The proposed GranSAM model excels in delivering segmentation masks with a user-centric approach, focusing on the desired granularity. Unlike SAM, which outputs numerous masks without labels, our strategy is targeted and meaningful. Instead of overwhelming users with an abundance of masks, GranSAM provides specific masks for user-defined objects, complete with meaningful labels. This user-centric approach to tailoring the granularity of object masks optimizes the user experience and enhances the interpretability of results, aligning with real-world scenarios where users seek specific objects within an image, consequently making the segmentation process more usable.

Ablation Study In our ablation study, we investigated the impact of introducing Uncertainty Distillation ($\mathcal{L}_{uncertainty}$) alongside the MIL loss (\mathcal{L}_{MIL}) in our classifier head (θ) training framework. The primary objective was to understand the performance implications of leveraging uncertainty information during training, particularly in challenging scenarios. The results obtained for the PASCAL VOC and COCO-80 datasets are tabulated in Tables 4 and 5 respectively.

Our experiments yielded compelling results, showcasing significant performance improvements, particularly in the PASCAL VOC dataset (with a +5% increase in mIoU and +6.59% in mAP₅₀) when leveraging web-crawled data for training. The strategic incorporation of Uncertainty Distil-

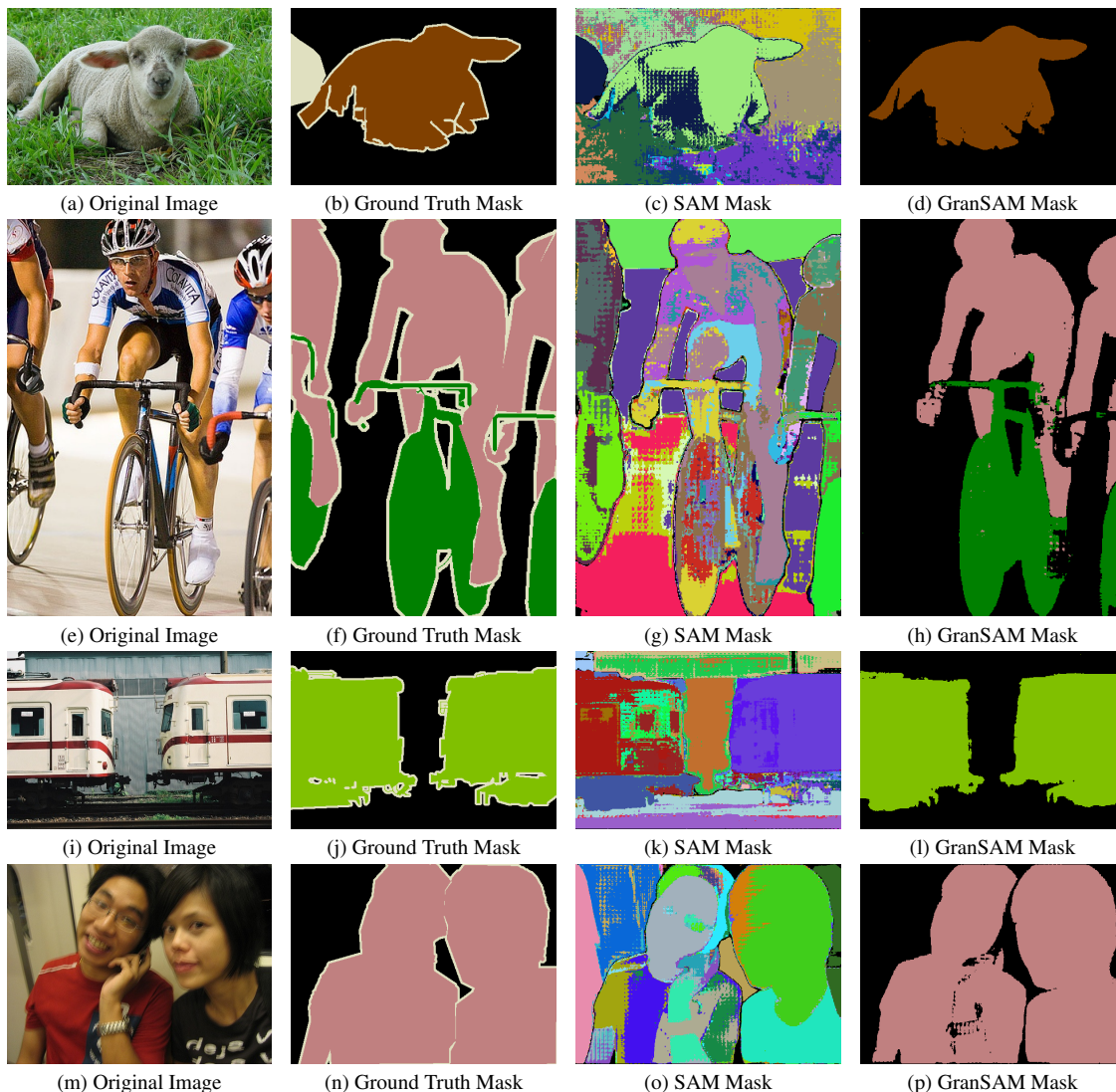


Figure 3. Qualitative results of GranSAM on the Pascal VOC Dataset: The original image, the ground truth mask, all of the SAM generated masks overlaid on top of each other, and the masks predicted by GranSAM are shown respectively in the four columns. For the ground truth and predicted masks, the colours indicate the class label, while random colours were used for the SAM masks since SAM does not provide class-labels.

lation alongside the MIL loss played a pivotal role in enhancing the model’s discriminative capabilities. Notably, this improvement is pronounced in the case of COCO-80, where the utilization of web-crawled training data addresses the challenges posed by the dataset’s diversity and complexity. The model’s adept handling of uncertainties in predictions proves crucial in navigating the intricacies of real-world scenarios presented by the diverse COCO-80 dataset.

A key observation is the model’s improved robustness in scenarios where traditional methods might struggle, showcasing the practical relevance of incorporating Uncertainty Distillation. The ability to make well-calibrated predictions and acknowledge uncertainties translated into a more effective and reliable segmentation framework.

5. Conclusion

In conclusion, GranSAM revolutionizes semantic segmentation annotation by automating pixel-level annotations and semantic masks, eliminating the need for labor-intensive manual labeling. Unlike traditional unsupervised methods, our innovative framework leverages SAM, a domain-agnostic foundation model pretrained on diverse data. The introduction of a classifier head atop SAM’s mask decoder, trained with synthetic/web-crawled images, enhanced the recognition of different regions based on semantics on an unseen test data at the granularity level defined by the user. Such a system provides a more efficient and flexible solution for annotation in semantic segmentation.

References

- [1] Rodrigo Benenson, Stefan Popov, and Vittorio Ferrari. Large-scale interactive object segmentation with human annotators. In *Proceedings of the IEEE/CVF conference on computer vision and pattern recognition*, pages 11700–11709, 2019. 2
- [2] Steve Branson, Grant Van Horn, and Pietro Perona. Lean crowdsourcing: Combining humans and machines in an online system. In *Proceedings of the IEEE Conference on Computer Vision and Pattern Recognition*, pages 7474–7483, 2017. 2
- [3] Mathilde Caron, Ishan Misra, Julien Mairal, Priya Goyal, Piotr Bojanowski, and Armand Joulin. Unsupervised learning of visual features by contrasting cluster assignments. *Advances in neural information processing systems*, 33:9912–9924, 2020. 6
- [4] Jang Hyun Cho, Utkarsh Mall, Kavita Bala, and Bharath Hariharan. Picie: Unsupervised semantic segmentation using invariance and equivariance in clustering. In *Proceedings of the IEEE/CVF Conference on Computer Vision and Pattern Recognition*, pages 16794–16804, 2021. 1, 2
- [5] Alexey Dosovitskiy, Lucas Beyer, Alexander Kolesnikov, Dirk Weissenborn, Xiaohua Zhai, Thomas Unterthiner, Mostafa Dehghani, Matthias Minderer, Georg Heigold, Sylvain Gelly, et al. An image is worth 16x16 words: Transformers for image recognition at scale. *arXiv preprint arXiv:2010.11929*, 2020. 3, 4
- [6] M. Everingham, L. Van Gool, C. K. I. Williams, J. Winn, and A. Zisserman. The PASCAL Visual Object Classes Challenge 2012 (VOC2012) Results. <http://www.pascal-network.org/challenges/VOC/voc2012/workshop/index.html>. 5
- [7] Shanghua Gao, Zhong-Yu Li, Ming-Hsuan Yang, Ming-Ming Cheng, Junwei Han, and Philip Torr. Large-scale unsupervised semantic segmentation. *IEEE transactions on pattern analysis and machine intelligence*, 2022. 2
- [8] Kaiming He, Haoqi Fan, Yuxin Wu, Saining Xie, and Ross Girshick. Momentum contrast for unsupervised visual representation learning. In *Proceedings of the IEEE/CVF conference on computer vision and pattern recognition*, pages 9729–9738, 2020. 6
- [9] Alexander Kirillov, Eric Mintun, Nikhila Ravi, Hanzi Mao, Chloe Rolland, Laura Gustafson, Tete Xiao, Spencer Whitehead, Alexander C Berg, Wan-Yen Lo, et al. Segment anything. *arXiv preprint arXiv:2304.02643*, 2023. 1, 2, 3
- [10] Feng Li, Hao Zhang, Peize Sun, Xueyan Zou, Shilong Liu, Jianwei Yang, Chunyuan Li, Lei Zhang, and Jianfeng Gao. Semantic-sam: Segment and recognize anything at any granularity. *arXiv preprint arXiv:2307.04767*, 2023. 2
- [11] Kehan Li, Zhennan Wang, Zesen Cheng, Runyi Yu, Yian Zhao, Guoli Song, Chang Liu, Li Yuan, and Jie Chen. Acseg: Adaptive conceptualization for unsupervised semantic segmentation. In *Proceedings of the IEEE/CVF Conference on Computer Vision and Pattern Recognition*, pages 7162–7172, 2023. 2, 6
- [12] Yuan-Hong Liao, Amlan Kar, and Sanja Fidler. Towards good practices for efficiently annotating large-scale image classification datasets. In *Proceedings of the IEEE/CVF Conference on Computer Vision and Pattern Recognition*, pages 4350–4359, 2021. 2
- [13] Tsung-Yi Lin, Michael Maire, Serge Belongie, James Hays, Pietro Perona, Deva Ramanan, Piotr Dollár, and C Lawrence Zitnick. Microsoft coco: Common objects in context. In *Computer Vision–ECCV 2014: 13th European Conference, Zurich, Switzerland, September 6–12, 2014, Proceedings, Part V 13*, pages 740–755. Springer, 2014. 5
- [14] Huan Ling, Jun Gao, Amlan Kar, Wenzheng Chen, and Sanja Fidler. Fast interactive object annotation with curve-gcn. In *Proceedings of the IEEE/CVF conference on computer vision and pattern recognition*, pages 5257–5266, 2019. 2
- [15] Shilong Liu, Zhaoyang Zeng, Tianhe Ren, Feng Li, Hao Zhang, Jie Yang, Chunyuan Li, Jianwei Yang, Hang Su, Jun Zhu, et al. Grounding dino: Marrying dino with grounded pre-training for open-set object detection. *arXiv preprint arXiv:2303.05499*, 2023. 2
- [16] Luca Medeiros. lang-segment-anything. <https://github.com/luca-medeiros/lang-segment-anything>, 2023. 2
- [17] Luke Melas-Kyriazi, Christian Rupprecht, Iro Laina, and Andrea Vedaldi. Deep spectral methods: A surprisingly strong baseline for unsupervised semantic segmentation and localization. In *Proceedings of the IEEE/CVF Conference on Computer Vision and Pattern Recognition*, pages 8364–8375, 2022. 1, 2
- [18] Alec Radford, Jong Wook Kim, Chris Hallacy, Aditya Ramesh, Gabriel Goh, Sandhini Agarwal, Girish Sastry, Amanda Askell, Pamela Mishkin, Jack Clark, et al. Learning transferable visual models from natural language supervision. In *International conference on machine learning*, pages 8748–8763. PMLR, 2021. 2
- [19] IDEA Research. Grounded segment anything. <https://github.com/IDEA-Research/Grounded-Segment-Anything>, 2023. 2
- [20] Robin Rombach, Andreas Blattmann, Dominik Lorenz, Patrick Esser, and Björn Ommer. High-resolution image synthesis with latent diffusion models. In *Proceedings of the IEEE/CVF Conference on Computer Vision and Pattern Recognition (CVPR)*, pages 10684–10695, 2022. 1
- [21] Robin Rombach, Andreas Blattmann, Dominik Lorenz, Patrick Esser, and Björn Ommer. High-resolution image synthesis with latent diffusion models. In *Proceedings of the IEEE/CVF conference on computer vision and pattern recognition*, pages 10684–10695, 2022. 3, 4, 5
- [22] Hyun Seok Seong, WonJun Moon, SuBeen Lee, and Jae-Pil Heo. Leveraging hidden positives for unsupervised semantic segmentation. In *Proceedings of the IEEE/CVF Conference on Computer Vision and Pattern Recognition*, pages 19540–19549, 2023. 2
- [23] Yonglong Tian, Chen Sun, Ben Poole, Dilip Krishnan, Cordelia Schmid, and Phillip Isola. What makes for good views for contrastive learning? *Advances in neural information processing systems*, 33:6827–6839, 2020. 6
- [24] Wouter Van Gansbeke, Simon Vandenhende, Stamatios Georgoulis, and Luc Van Gool. Unsupervised semantic seg-

- mentation by contrasting object mask proposals. In *Proceedings of the IEEE/CVF International Conference on Computer Vision*, pages 10052–10062, 2021. 2, 6
- [25] Ashish Vaswani, Noam Shazeer, Niki Parmar, Jakob Uszkoreit, Llion Jones, Aidan N Gomez, Łukasz Kaiser, and Illia Polosukhin. Attention is all you need. *Advances in neural information processing systems*, 30, 2017. 4
- [26] Antonin Vobecky, David Hurych, Oriane Siméoni, Spyros Gidaris, Andrei Bursuc, Patrick Pérez, and Josef Sivic. Drive&segment: Unsupervised semantic segmentation of urban scenes via cross-modal distillation. In *European Conference on Computer Vision*, pages 478–495. Springer, 2022. 1, 2
- [27] Haosen Yang, Chuofan Ma, Bin Wen, Yi Jiang, Zehuan Yuan, and Xiatian Zhu. Recognize any regions. *arXiv preprint arXiv:2311.01373*, 2023. 2
- [28] Zhaoyuan Yin, Pichao Wang, Fan Wang, Xianzhe Xu, Hanling Zhang, Hao Li, and Rong Jin. Transfgu: a top-down approach to fine-grained unsupervised semantic segmentation. In *European conference on computer vision*, pages 73–89. Springer, 2022. 6, 7
- [29] Haoxuan You, Haotian Zhang, Zhe Gan, Xianzhi Du, Bowen Zhang, Zirui Wang, Liangliang Cao, Shih-Fu Chang, and Yinfei Yang. Ferret: Refer and ground anything anywhere at any granularity. *arXiv preprint arXiv:2310.07704*, 2023. 1
- [30] Andrii Zadaianchuk, Matthaeus Kleindessner, Yi Zhu, Francesco Locatello, and Thomas Brox. Unsupervised semantic segmentation with self-supervised object-centric representations. *arXiv preprint arXiv:2207.05027*, 2022. 2
- [31] Daoan Zhang, Chenming Li, Haoquan Li, Wenjian Huang, Lingyun Huang, and Jianguo Zhang. Rethinking alignment and uniformity in unsupervised image semantic segmentation. In *Proceedings of the AAAI Conference on Artificial Intelligence*, pages 11192–11200, 2023. 1, 2
- [32] Adrian Ziegler and Yuki M Asano. Self-supervised learning of object parts for semantic segmentation. In *Proceedings of the IEEE/CVF Conference on Computer Vision and Pattern Recognition*, pages 14502–14511, 2022. 6, 7

Supplementary Information

This supplementary document complements the main manuscript by providing additional insights and details that enhance the understanding of our proposed GranSAM model. Here, we offer a closer look at specific aspects, addressing nuances and expanding on key elements mentioned in the primary text. The supplementary content includes:

- **Examples of Stable Diffusion Images** (Section 1): Explore the limitations of Stable Diffusion in generating realistic multi-object images and its proficiency when focused on a single salient object.
- **Architecture of Classifier Head** (Section 2): Gain a deeper understanding of the classifier head’s architecture in GranSAM. Detailed layer-wise information is provided, shedding light on the network’s inner workings.
- **Additional Experiments** (Section 3): Delve into further experiments and comparisons. This section includes additional comparisons with baseline methods, classwise mIoU results for COCO-80 using GranSAM, and qualitative results showcasing the impact of changed granularity in our approach.
- **Failure Cases** (Section 5): Investigate instances where GranSAM faced challenges and failed to correctly annotate objects in images. This section provides valuable insights into the model’s limitations and areas for potential improvement.

1. Examples of Stable Diffusion Images

We utilized Stable Diffusion-v1-4 [?] to generate synthetic images for training the GranSAM model. While Stable Diffusion excels at creating hyper-realistic single-object images, its performance falters when generating realistic multi-object scenes. Examples of images generated with Stable Diffusion are showcased in Figure 1. In (a), prompted with “dog with aeroplane,” the model produces an image featuring two aeroplanes without any dogs. While it’s true that instances of a “dog” with an “aeroplane” are uncommon, in (b) with the prompt “person with dog,” where such combinations are frequent, Stable Diffusion fails to produce a convincing image, superimposing a dog on the person. Similarly, in (c) with the prompt “person with truck,” a single-object “truck” image is generated, omitting the “person” object. In parts (d)-(e), where the prompt highlights a single salient object, Stable Dif-

Layer Name	Input Dimension	Output Dimension
f_c	$d \times 1024$	$d \times 512$
f_{c1}	$d \times 512$	$d \times 256$
f_{c2}	$d \times 256$	$d \times 128$
f_{c3}	$d \times 128$	$d \times C$

Table 1. Architectural details of the classifier head θ of GranSAM. d is the number of predicted masks per image by SAM [?] and C is the number of user-defined object classes.

fusion successfully generates realistic images suitable for GranSAM training.

2. Architecture of Classifier Head

As detailed in the main manuscript, the classifier head θ of GranSAM comprises a 4-layer network. Table 1 provides a breakdown of the layer-wise specifications for θ . The activation function ReLU is applied to layers f_c , f_{c1} , and f_{c2} , with an additional dropout regularization on layer f_{c2} , employing a dropout probability of 90%. This dropout regularization is implemented to prevent overfitting to synthetic or web crawled image data, ensuring robust generalization to the actual test data distribution.

3. Additional Experiments

3.1. Baseline Comparison

We configured Leopot [?] as a baseline method, training it on synthetic or web-crawled data and evaluating its performance on the PASCAL VOC or COCO-80 datasets. Additionally, we included Leopot’s performance when trained on the *train* sets of PASCAL VOC and COCO-80, tested on their respective *val* sets. The results are compared to our GranSAM and presented in Tables 2 and 3 for the PASCAL VOC and COCO-80 datasets, respectively.

As an additional baseline, we incorporated the CLIP [?] model, renowned for its zero-shot performance. The baseline setup for CLIP involves computing the similarity between images and a set of natural language words/phrases, leveraging its shared Vision-Language embedding space. Utilizing the d masks predicted by SAM for each image, we generate d pooled images, with each corresponding to a distinct object category. Subsequently, we calculate the



Figure 1. Illustrative examples of images generated by Stable Diffusion [?], corresponding to prompts mentioned in the captions. Stable Diffusion fails to generate realistic images when the given prompt involves more than one salient object.

Table 2. Baseline Results on PASCAL VOC

Method	Training Data			mIoU	mAP ₅₀
	PASCAL	Synthetic	Web crawl		
Leopart [?]	✓			23.28%	-
Leopart [?]		✓		7.21%	-
GranSAM		✓		25.16%	49.06%
Leopart [?]			✓	6.79%	-
GranSAM			✓	22.42%	45.59%

Table 3. Baseline Results on COCO-80

Method	Training Data			mIoU	mAP ₅₀
	COCO	Synthetic	Web crawl		
Leopart [?]	✓			6.91%	-
Leopart [?]		✓		3.84%	-
GranSAM		✓		8.60%	30.90%
Leopart [?]			✓	3.81%	-
GranSAM			✓	9.01%	31.80%

similarity between all d pooled images and each of the C user-defined object classes. Similar to our GranSAM post-processing, we set a similarity threshold at 70% and apply Non-Maximal Suppression to retain only unique objects while eliminating redundant masks. The results obtained by CLIP [?] compared to our GranSAM model are reported in Table 4.

3.2. Class-wise mIoU for COCO-80

The class-wise mIoU results obtained by GranSAM on the COCO-80 dataset, when trained on synthetic images are reported in Table 5 and when trained on web crawled images are reported in Table 6.

Table 4. Comparison of GranSAM performance with CLIP [?] on the PASCAL VOC and COCO-80 datasets.

Method	mIoU	mAP ₅₀
<i>PASCAL VOC</i>		
CLIP [?]	19.17%	42.45%
GranSAM	25.16%	49.06%
<i>COCO-80</i>		
CLIP [?]	7.91%	29.93%
GranSAM	9.01%	31.80%

4. Results with Changed Granularity

We modified the class definitions for the PASCAL VOC dataset to adjust the granularity of user-defined classes. Specifically, we introduced some superset classes that encompass several PASCAL VOC classes together. The revised class definitions and the corresponding PASCAL VOC classes falling into these categories are as follows:

1. animals: “bird”, “cat”, “cow”, “dog”, “horse”, “sheep”
2. furniture: “chair”, “diningtable”, “sofa”
3. household items: “bottle”, “pottedplant”, “tvmonitor”
4. person: “person”
5. transportation: “aeroplane”, “bicycle”, “boat”, “bus”, “car”, “motorbike”, “train”

We employed the GranSAM model to assess the PASCAL VOC dataset with the refined class definitions. For each of the five new classes, we generated 200 synthetic images using the Stable Diffusion model, extracted SAM mask embeddings m_i for each image, and trained the clas-

Class Name	Background	Airplane	Apple	Backpack	Banana	Baseball Bat	Baseball Glove	Bear	Bed
mIoU (%)	74.47	22.71	0.11	0.00	4.21	0.00	0.00	18.85	4.63
Class Name	Bench	Bicycle	Bird	Boat	Book	Bottle	Bowl	Broccoli	Bus
mIoU (%)	6.78	19.80	6.06	8.68	1.25	2.16	4.63	13.79	28.64
Class Name	Cake	Car	Carrot	Cat	Cell Phone	Chair	Clock	Couch	Cow
mIoU (%)	6.30	4.66	7.37	5.86	5.57	11.52	3.99	2.29	7.37
Class Name	Cup	Dining Table	Dog	Donut	Elephant	Fire Hydrant	Fork	Frisbee	Giraffe
mIoU (%)	3.24	10.89	13.09	2.31	22.87	26.41	0.00	0.00	35.87
Class Name	Hair Dryer	Handbag	Horse	Hot Dog	Keyboard	Kite	Knife	Laptop	Microwave
mIoU (%)	0.00	0.00	7.74	4.74	12.43	0.00	0.00	5.85	9.47
Class Name	Motorcycle	Mouse	Orange	Oven	Parking Meter	Person	Pizza	Potted Plant	Refrigerator
mIoU (%)	45.43	0.00	8.13	3.69	7.85	19.22	22.05	3.64	11.27
Class Name	Remote	Sandwich	Scissors	Sheep	Sink	Skateboard	Skis	Snowboard	Spoon
mIoU (%)	0.77	11.79	2.35	12.51	1.09	2.68	0.03	0.01	0.00
Class Name	Sports Ball	Stop Sign	Suitcase	Surfboard	Teddy Bear	Tennis Racket	Tie	Toaster	Toilet
mIoU (%)	0.00	36.09	6.44	0.00	21.39	0.04	0.84	0.00	6.12
Class Name	Toothbrush	Traffic Light	Train	Truck	TV	Umbrella	Vase	Wine Glass	Zebra
mIoU (%)	0.00	6.81	15.03	8.43	9.52	0.00	3.26	6.57	48.18

Table 5. Class-wise mIoU Scores obtained by GranSAM on the COCO-80 dataset when trained with the *synthetic dataset*.

Class Name	Background	Airplane	Apple	Backpack	Banana	Baseball Bat	Baseball Glove	Bear	Bed
mIoU (%)	74.47	22.71	0.11	0.00	4.21	0.00	0.00	18.85	4.63
Class Name	Bench	Bicycle	Bird	Boat	Book	Bottle	Bowl	Broccoli	Bus
mIoU (%)	6.78	19.80	6.06	8.68	1.25	2.16	4.63	13.79	28.54
Class Name	Cake	Car	Carrot	Cat	Cell Phone	Chair	Clock	Couch	Cow
mIoU (%)	6.30	4.66	7.37	5.86	5.57	11.52	3.99	2.29	7.37
Class Name	Cup	Dining Table	Dog	Donut	Elephant	Fire Hydrant	Fork	Frisbee	Giraffe
mIoU (%)	3.24	10.89	13.09	5.86	22.87	26.41	0.00	0.01	35.87
Class Name	Hair Dryer	Handbag	Horse	Hot Dog	Keyboard	Kite	Knife	Laptop	Microwave
mIoU (%)	0.00	0.00	7.74	4.74	12.43	0.00	0.00	5.85	9.47
Class Name	Motorcycle	Mouse	Orange	Oven	Parking Meter	Person	Pizza	Potted Plant	Refrigerator
mIoU (%)	45.37	0.00	8.13	3.69	7.85	19.22	22.05	3.64	11.27
Class Name	Remote	Sandwich	Scissors	Sheep	Sink	Skateboard	Skis	Snowboard	Spoon
mIoU (%)	0.77	11.79	2.35	12.51	1.09	2.68	0.03	0.01	0.00
Class Name	Sports Ball	Stop Sign	Suitcase	Surfboard	Teddy Bear	Tennis Racket	Tie	Toaster	Toilet
mIoU (%)	0.00	36.09	6.44	0.00	21.39	0.04	0.84	0.00	6.12
Class Name	Toothbrush	Traffic Light	Train	Truck	TV	Umbrella	Vase	Wine Glass	Zebra
mIoU (%)	0.00	6.81	15.03	8.43	9.52	0.00	3.26	6.57	48.18

Table 6. Class-wise mIoU Scores obtained by GranSAM on the COCO-80 dataset when trained with the *web crawled dataset*.

sifier head θ . With this updated granularity configuration, we achieved an mAP₅₀ score of 61.54%.

Qualitative results are depicted in Figure 2, where Row-1 and Row-2 showcase correct segmentation of objects (“aeroplane” and “train”) from the same class, “transportation.” In Row-3, a “sheep” object is depicted, and in Row-4, there are two objects, “dog” and “cat,” both now categorized under “animals” with the renewed class definitions, demonstrating accurate segmentation by GranSAM. Row-4 illustrates an example of the “person” class, while Row-5 exhibits an instance of the “furniture” class object.

5. Failure Cases

Figure 3 illustrates instances where GranSAM encountered challenges in generating accurate annotations.

- Row-1: Presents a scenario where objects belonging to the “bird” class were mislabeled as “zebra.” The intricate

details of bird wings, a salient feature for the “bird” category, were challenging to distinguish, and the black and white feathers, resembling a zebra’s pattern, led to the misclassification.

- Row-2: Exhibits a similar case where the class “bed” was predicted as “couch”. The semantic similarities between these furniture items, including pillows that can be mistaken for cushions on a couch, contributed to the misclassification.
- Row-3: Highlights an example with the actual object class being “donut”. However, in the predictions, only one of the three “donut” objects was correctly classified, while the other two were mislabeled as “sandwich.” This discrepancy arose due to the semantic similarity between the pink-colored donut and a sandwich, leading to misinterpretation.

These instances underscore the model’s susceptibility to

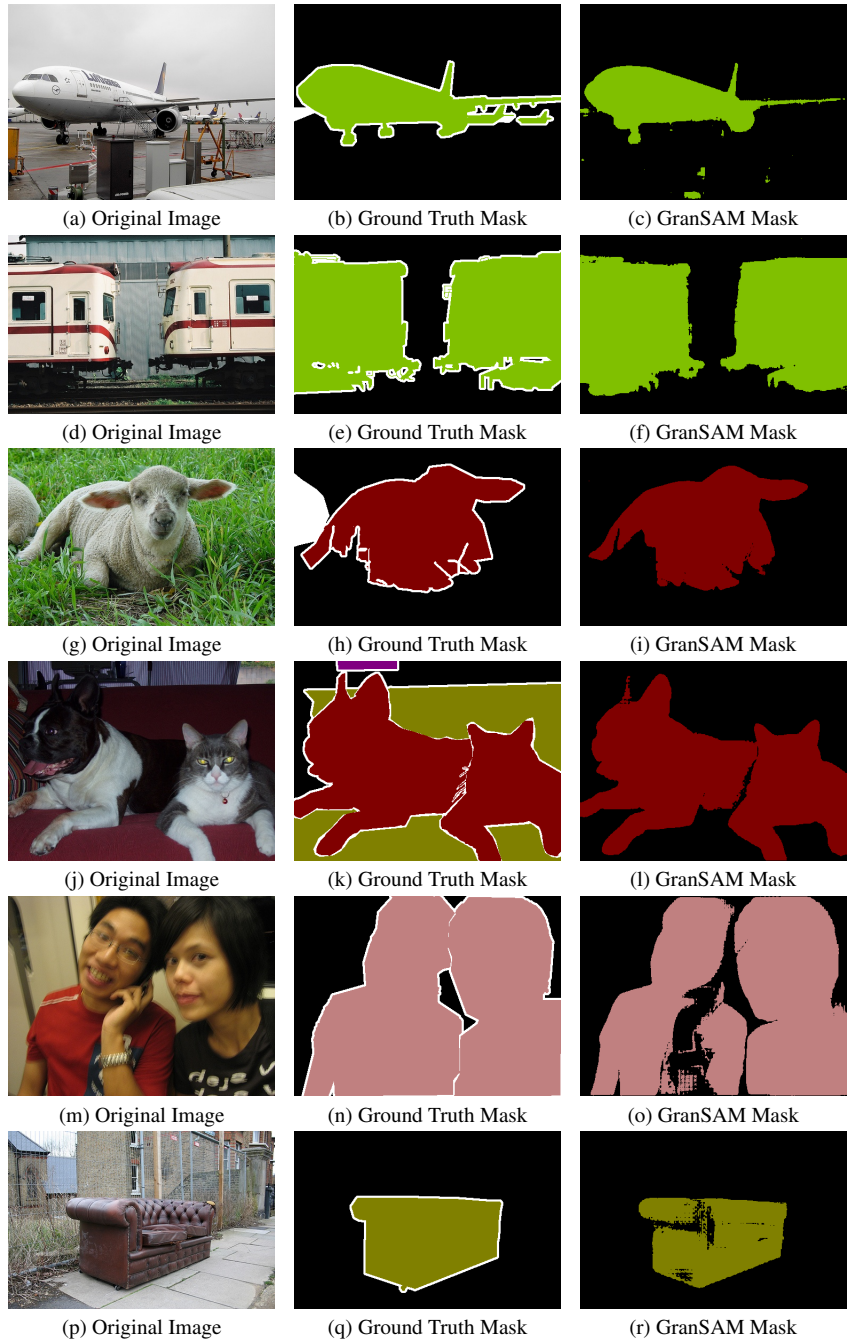


Figure 2. Qualitative results obtained by GranSAM, when the PASCAL VOC dataset classes were updated to change the granularity level. The colours represent the different object classes.

semantic similarities between object classes, revealing areas for potential improvement in handling nuanced distinctions. Moreover, the consistent spatial accuracy of the generated semantic masks suggests that GranSAM effectively captures the relevant regions, even when faced with challenges in label assignment.



Figure 3. Examples of cases where GranSAM failed to generate correct annotations. The different colors in the masks represent the different class labels.